Since January 2020 Elsevier has created a COVID-19 resource centre with free information in English and Mandarin on the novel coronavirus COVID-19. The COVID-19 resource centre is hosted on Elsevier Connect, the company's public news and information website.

The MiR-17-92 Gene Cluster is a Blood-Based Marker for Cancer Detection in Non-Small-Cell Lung Cancer

Chenghao Yang, BE[1], Xiaoyu Jia, BE[1], Jinbao Zhou, MS[1], Qiangling Sun, PhD[2] and Zhongliang Ma, PhD[1]

[1] Lab for Noncoding RNA & Cancer, School of Life Sciences, Shanghai University, Shanghai, China; [2] Department of Thoracic Surgery, Thoracic Cancer Institute, Shanghai Chest Hospital Affiliated to Shanghai Jiao Tong University, Shanghai, China

ABSTRACT

Background: Lung cancer is one of the most malignant cancers threatening human health. The miR-17-92 gene cluster is a highly conserved oncogene cluster encoding 6 miRNAs: miR-17, miR-18a, miR-19a, miR-19b-1, miR-20a and miR-92a. This study explored whether these miRNAs can be used as diagnostic markers for non-small-cell lung cancer (NSCLC).

Methods: Serum samples were collected from healthy subjects (n = 23) and NSCLC patients at various stages (n = 74). Serum RNA was extracted by the TRIzol-glycogen method, and cDNA libraries were constructed by reverse transcription. Quantitative real-time polymerase chain reaction (qRT-PCR) was utilized to detect the expression levels of the 6 miRNAs.

Results: The expression levels of the 6 miRNAs varied in different stages of NSCLC. Thus, 2 receiver operating characteristic (ROC) curves, that is, normal subjects and stage I-III patients and normal subjects and stage IV patients, of each miRNA were established to determine the interval of normal ΔCt values. The 2 areas under the curve (AUCs) of each miRNA were investigated (miR-17: 0.8097 and 1.000; miR-18a: 0.7388 and 0.9907; miR-19a/19b: 0.8451 and 0.5104; miR-20a: 0.8975 and 1.000; miR-92a: 0.8097 and 0.8342). In addition, a high positive correlation was discovered between miR-17 and miR-20a expression. Combining these 2 miRNAs can improve the screening effect of NSCLC.

Conclusion: The miR-17-92 gene cluster can likely serve as a diagnostic marker in NSCLC.

Key Indexing Terms: miR-17-92 gene cluster; Non-small-cell lung cancer; Diagnostic markers. **[Am J Med Sci 2020;360 (3):248–260.]**

INTRODUCTION

Among all cancers, lung cancer is one of most malignant cancers, with its incidence ranking second and its mortality rate ranking first.[1] Lung cancer has 2 main types, small-cell lung cancer (SCLC) and non-small-cell lung cancer (NSCLC),[2] the latter accounting for 85% of lung cancer.[3] Both of them have a low 5-year survival rate. In the United States, the 5-year survival rate of lung cancer is only 17.4%,[4] and this value is even lower in developing countries. Therefore, lung cancer is one of the most serious diseases threatening human health.[1]

MiRNAs are small RNA molecules containing 19-22 nucleotides found in plants, animals and some viruses.[5] They are paramount in maintaining the function of normal cells. They also have special traits such as tissue specificity, high conservation and changes with time.[6] The atypical expression of miRNAs may induce many diseases, including tumorigenesis, such as lung cancer, liver cancer, and breast cancer.[7,8] Therefore, the regulation of miRNAs in malignant tumors provides a new direction for the prevention and treatment of tumors.[9,10] Studies have revealed that miRNAs play a preponderant role in tumor development, metastasis, invasion and treatment.[11] The aberrant expression of some miRNAs may be harnessed as early diagnostic markers in patients who have cancer.[12]

The miR-17-92 gene cluster[13,14] is a highly conserved gene cluster containing 6 members: miR-17, miR-18a, miR-19a, miR-19b-1, miR-20a and miR-92a-1.[15] This gene cluster is the first discovered cluster of miRNA oncogenes.[16,17] In this study, sequences with higher expression levels in the -3p and -5p sequences of each miRNA in the miR-17-92 gene cluster were selected (Table 1). Among them, miR-19a-3p has exactly the same sequence as miR-19b-1-3p.[18] The miRNAs below, if not indicated by -3p/-5p, are default to the miRNAs shown in Table 1.

Studies have revealed that the miR-17-92 gene cluster plays an important role in the occurrence and

TABLE 1. Sequences with higher expressions of the miR-17-92 gene cluster.

Name of miRNA	Sequence
hsa-miR-17-5p	CAA AGU GCU UAC AGU GCA GGU AG
hsa-miR-18a-5p	UAA GGU GCA UCU AGU GCA GAU AG
hsa-miR-19a-3p	UGU GCA AAU CUA UGC AAA ACU GA
hsa-miR-19b-1-3p	UGU GCA AAU CCA UGC AAA ACU GA
hsa-miR-20a-5p	UAA AGU GCU UAU AGU GCA GGU AG
hsa-miR-92a-1-3p	UAU UGC ACU UGU CCC GGC CUG U

development of a variety of tumors.[19,20] For this reason, it has received extensive attention from researchers around the world. Liu et al found that miR-17-92 regulates the NF-kappa B signaling pathway by targeting TNF receptor-associated factor 3 (TRAF3) to promote gastric cancer.[21] Jia et al found that miR-17-92 causes leukemia by targeting A20.[22] Zhou et al found that miR-17-92 promotes the development of prostate cancer and enables cancer cells to acquire the ability to resist chemotherapeutic drugs such as cisplatin.[23]

In a previous study, we discovered that miR-18a-5p in the miR-17-92 gene cluster directly targets interferon regulatory factor 2 (IRF2), prominently lowering the expression of its protein.[24] Since IRF2 has the ability to inhibit lung cancer cell growth, miR-18a-5p promotes the proliferation and migration of NSCLC by targeting IRF2. Our lab also investigated whether the miR-17-92 cluster promoted NSCLC by targeting the suppressor gene sprouty homolog 4 (SPRY4).

By querying the National Center for Biotechnology Information (NCBI) database, the roles of the miR-17-92 gene cluster in lung cancer were elucidated to a certain extent. Based on our previous research, this study explored the expression of the miR-17-92 cluster in the sera of NSCLC patients to screen for possible miRNAs that can be used as diagnostic markers for NSCLC in the clinic.[25] The diagnostic effects of the existing clinical markers of NSCLC were then compared with those of the miRNAs.[26] Our findings may provide new ideas for improving the clinical screening and diagnosis of NSCLC and thus promoting the precise treatment of lung cancer.[27]

MATERIALS AND METHODS

Study Design and Serum Samples

Our procedures were approved by the Ethics Review Board of Shanghai Chest Hospital Affiliated to Shanghai Jiao Tong University, and written informed consent was obtained.

Sera were collected from 97 subjects, including 74 NSCLC patients (from stage I to IV) and 23 normal subjects from the Shanghai Chest Hospital.

In this study, various procedures were performed (Figure 1). Serum RNA was extracted by the TRIzol-glycogen method, and then cDNA libraries were constructed by reverse transcription (SYBR Prime Script miRNA RT-PCR Kit, TaKaRa Bio, Shibuya, Japan). Then, quantitative real-time polymerase chain reaction (qRT-PCR) (ChamQ SYBR qPCR Master Mix, Vazyme, Nanjing, China) was utilized to detect miRNA expression.

The receiver operating characteristic (ROC) curves of the 6 miRNAs were plotted. By observing the area under the curve (AUC), the diagnostic effect of the miRNAs could be judged. The value corresponding to the maximum of the Youden index, that is, sensitivity + specificity − 1, was taken as the best cut-off point.

Serum RNA Extraction

The total RNA of the serum samples were extracted using TRIzol (TranS, Beijing, China). Then, 30-50 μL of RNase-free ddH_2O was added to fully dissolve the RNA. The RNA solutions were stored at -70 °C for subsequent experiments. The concentration of total RNA was measured by a NanoDrop 2000 Spectrophotometer (Thermo Fisher Scientific, Waltham, MA). Serum samples whose concentration of total RNA was less than 20 ng/μL were excluded from this study.

Reverse Transcription and qRT-PCR

The reverse transcription solution was prepared according to the manufacturer's protocol (SYBR Prime Script miRNA RT-PCR Kit, TaKaRa Bio, Shibuya, Japan). The mixture was incubated at 37 °C for 60 minutes and then at 85 °C for 5 seconds to inactivate the enzyme. RNase-free ddH_2O was added to the obtained reverse transcription reaction solution to reach 100 μL.[28] The diluent was added to the qRT-PCR system for quantitative detection.[29,30] qRT-PCR solutions were prepared according to the manufacturer's protocol (ChamQ SYBR qPCR Master Mix, Vazyme, Nanjing, China). The qRT-PCR protocol was conducted on a CFX96 Touch Real-Time PCR Detection System (BIO-RAD, Hercules, CA) in 96-well plates at 95 °C for 3 minutes, followed by 42 cycles of 95 °C for 10 seconds and 55 °C for 30 seconds. A melt-curve was plotted to evaluate the specificity of the PCR product.[31] Cycle threshold (Ct) values less than 40 were used in this study.

The data are analyzed and compared by the $2^{-\Delta\Delta Ct}$ quantitative method relative to the reference RNU6B (U6), $\Delta Ct = Ct_{miRNA} - Ct_{U6}$.[32,33]

ROC Curve, AUC, and Youden Index

The ROC curve refers to the connection of points drawn under a specific cut-off point, with the false positive rate (1 − specificity) obtained by the subjects under different cut-off points as the abscissa and the true positive rate (sensitivity) as the ordinate.

In this study, we selected different ΔCt values of each miRNA as cut-off points, according to the qRT-PCR results. In stages I-III, several miRNAs are downregulated. In that case, ΔCt values greater than the cut-off point are regarded as positive, while ΔCt values less than the cut-off point are regarded as negative. In stage IV, all miRNAs

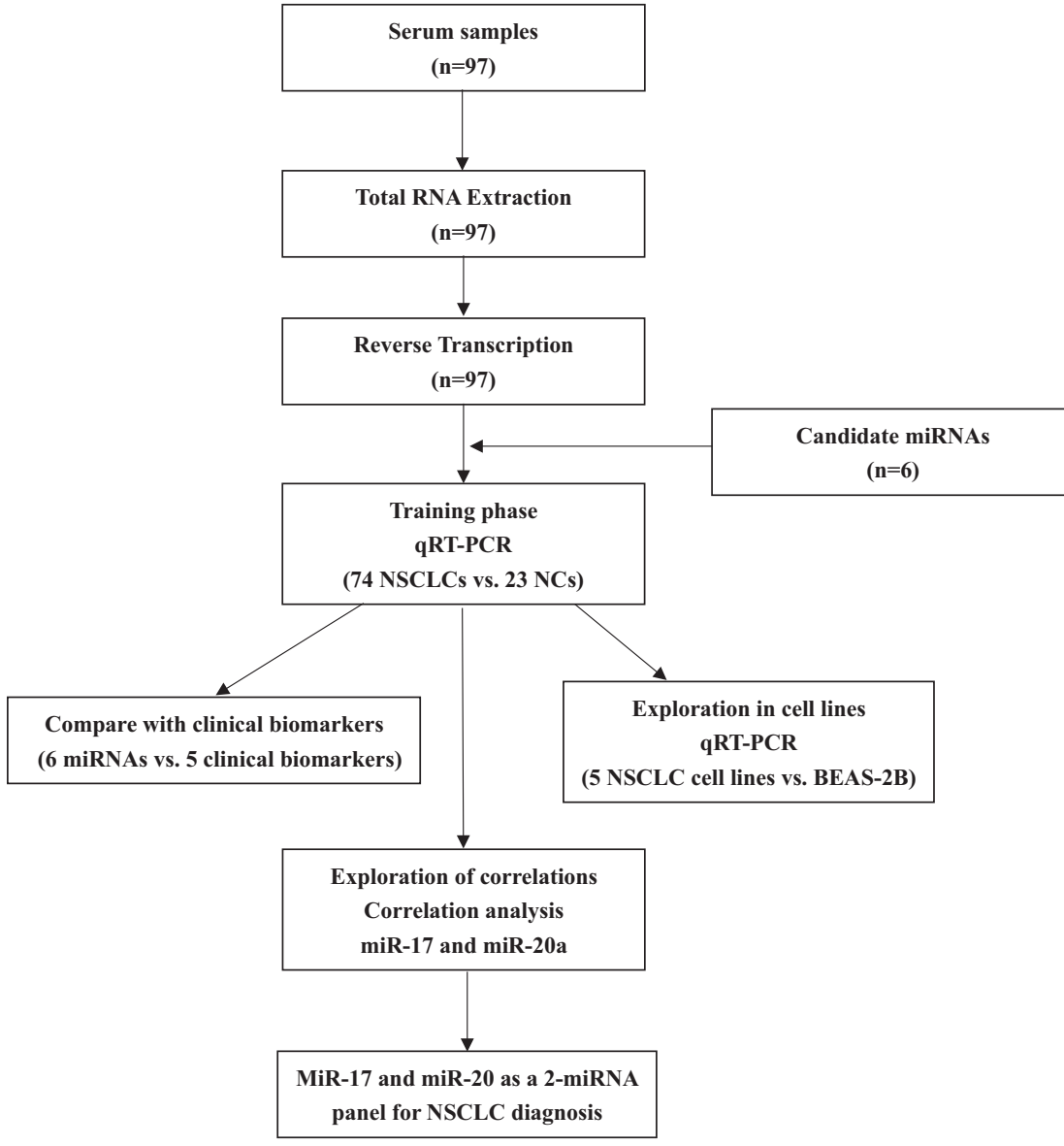

FIGURE 1. Flow chart of the experimental design. Abbreviations: NSCLC, non-small-cell lung cancer; NC, normal control; BEAS-2B, human bronchial epithelial cells.

are upregulated. Then ΔCt values greater than the cut-off point are regarded as negative, while ΔCt values less than the cut-off point are regarded as positive.

In the control group, the true negative rate (specificity) can be calculated as the "# of controls whose test result is negative / # of controls in total", while the false positive rate can be calculated as 1 − specificity. In the patient group, the true positive rate (sensitivity) can be calculated as the "# of patients whose test result is positive / # of patients in total," while the false negative rate can be calculated as 1 − sensitivity.

By connecting the points drawn under different cut-off points, the AUC can be determined. AUC is the area enclosed by the coordinate axis under the ROC curve. The closer the AUC is to 1, the better the discrimination effect of the detection method. Typically, an AUC greater than 0.8 indicates that the detection method has relatively good effects.

The best cut-off point is identified by the Youden index, which is sensitivity + specificity − 1. The Youden index represents the total ability of the screening method to find true patients and nonpatients. In this study, the cut-off point that has the maximum value of the Youden index was chosen as the best cut-off point.

Statistical Analysis

Unpaired *t* test was used to compare 2 groups of continuous variables. The diagnostic effect of the miRNAs was evaluated by ROC curves. Then, the AUCs

were calculated to compare the diagnostic value of each miRNA. The Pearson correlation coefficient was utilized to measure the degree of correlation between 2 continuous variables. The maximum Youden index, that is, sensitivity + specificity − 1, was taken as the best cut-off point. Binary logistic regression was used to create the prediction model for combining the diagnostic effects of multiple miRNAs together. The *P* value[34] was calculated for each statistical analysis to indicate whether the null hypothesis can be refuted.[33]

RESULTS

Characteristics of the Subjects

Serum samples from 23 normal subjects and 74 NSCLC patients were used in this study. The demographics and clinical characteristics of the patients with NSCLC are listed in Table S1. There was no significant difference in the sex or age distributions between the normal subjects and patients with NSCLC in different stages.

MiR-17

Compared with that of normal subjects, the level of miR-17 in NSCLC patients showed no significant change in stage I. In stage II and III patients, it showed significant downregulation, and in stage IV patients, it was markedly upregulated (Figure 2A). From this phenomenon, the ROC curve of normal subjects and stage I-III patients and the ROC curve of normal subjects and stage IV patients could be plotted. Then, the interval of normal human ΔCt values could be determined.

The ROC curve for normal subjects and stage I-III patients determines the upper limit of the ΔCt value, and

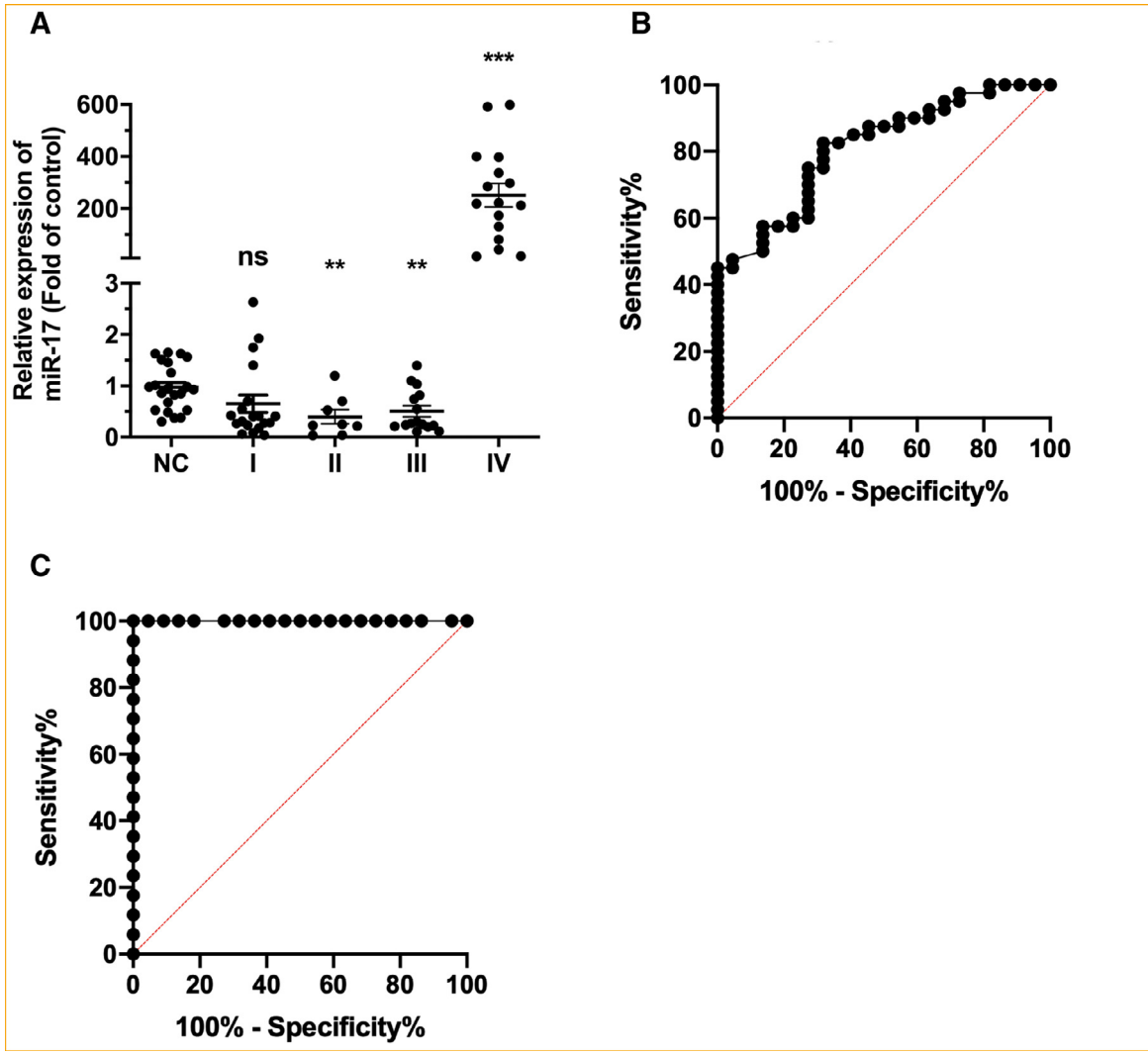

FIGURE 2. Expression level and ROC curve of miR-17 in the sera of NSCLC patients. (A) Expression level of miR-17 in the sera of NSCLC patients; (B) ROC curve of miR-17 in stage I-III patients; (C) ROC curve of miR-17 in stage IV patients. Abbreviations: NSCLC, non-small-cell lung cancer; ROC, receiver operating characteristic.

the ROC curve for normal subjects and stage IV patients determines the lower limit of the ΔCt value.

The results showed that in the ROC curve of normal subjects and stage I-III patients, the AUC was 0.8097, and the best cut-off point was 3.085. The sensitivity and specificity of this value were 0.8250 and 0.6818, respectively (Figure 2B). In the ROC curve of normal subjects and stage IV patients, the AUC was 1.0000, and the best cut-off point was -0.1317. The sensitivity and specificity of this value were 1.0000 (Figure 2C).

Therefore, the ΔCt value interval of a normal person can be set to [-0.1317, 3.085]. If the test result is less than -0.1317, it is suggested to be stage IV NSCLC; if the result is greater than 3.085, it is suggested to be stage I-III NSCLC.

MiR-18a

The expression level of miR-18a in NSCLC patients showed no significant change in stages I and III. In stage II patients, it showed significant downregulation, and in stage IV patients, it showed marked upregulation (Figure 3A). Although there was no significant change in stage I and III, patients with low expression still accounted for a considerable proportion. Therefore, the ROC curve of normal subjects and stage I-III patients

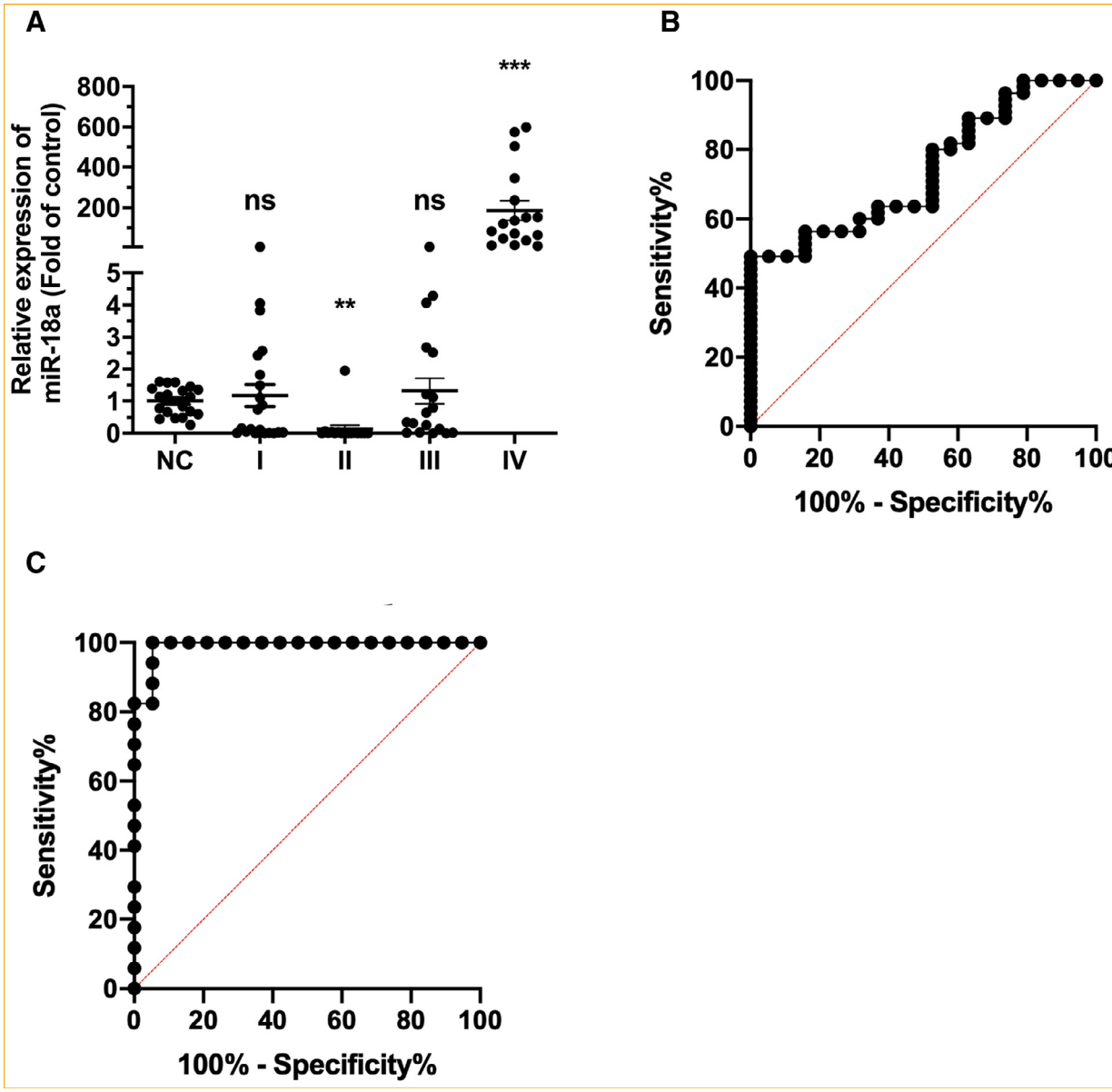

FIGURE 3. Expression level and ROC curve of miR-18a in the sera of NSCLC patients. (A) Expression level of miR-18a in the sera of NSCLC patients; (B) ROC curve of miR-18a in stage I-III patients; (C) ROC curve of miR-18a in stage IV patients. Abbreviations: NSCLC, non-small-cell lung cancer; ROC, receiver operating characteristic.

and the ROC curve of normal subjects and stage IV patients could be plotted. Then, the interval of normal human ΔCt values could be determined.

The results showed that in the ROC curve of normal subjects and stage I-III patients, the AUC was 0.7388, and the best cut-off point was 4.788. The sensitivity and specificity of this value were 0.8000 and 0.4737, respectively (Figure 3B). In the ROC curve of normal subjects and stage IV patients, the AUC was 0.9907, and the best cut-off point was 2.620. The sensitivity and specificity of this value were 1.0000 and 0.8947, respectively (Figure 3C).

In that case, the ΔCt value interval of a normal person can be set to [2.620, 4.788]. If the test result is less than 2.620, it is suggested to be stage IV NSCLC; if the result is greater than 4.788, it is suggested to be stage I-III NSCLC.

MiR-19a/19b

The expression level of miR-19a/19b in NSCLC patients showed no significant change in stages I and IV. In stage II and III patients, it was significantly downregulated (Figure 4A). The ROC curve of normal subjects and stage I-III patients and the ROC curve of normal subjects and stage IV patients were plotted.

The results showed that in the ROC curve of normal subjects and stage I-III patients, the AUC was 0.8451, and the best cut-off point was 4.270. The sensitivity and specificity of this value were 0.7885 and 0.5556, respectively (Figure 4B). In the ROC curve of normal subjects and stage IV patients, the AUC was only 0.5104, showing that there was almost no effect in the diagnosis of stage IV NSCLC patients using miR-19a/19b (Figure 4C).

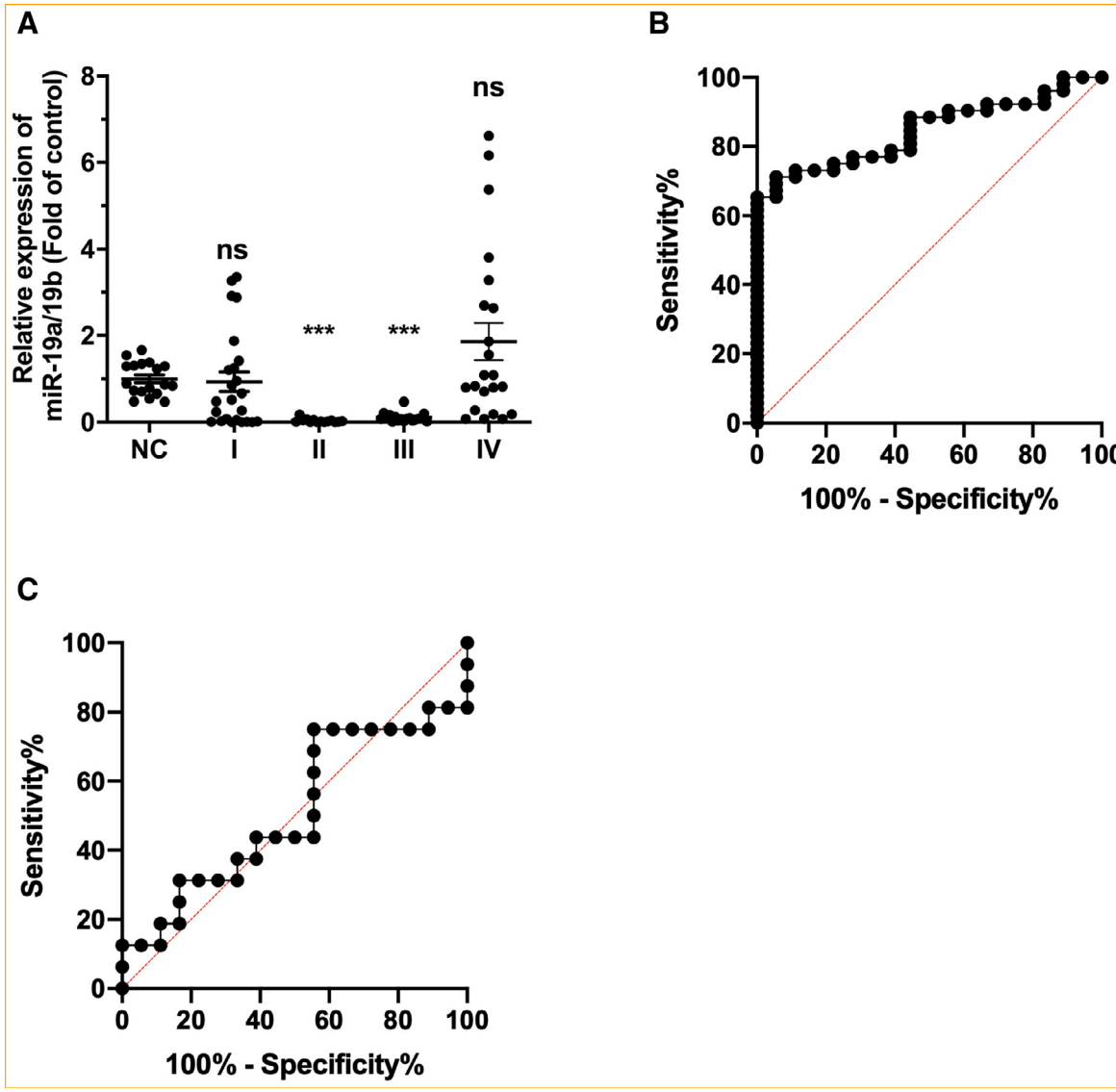

FIGURE 4. Expression level and ROC curve of miR-19a/19b in the sera of NSCLC patients. (A) Expression level of miR-19a/19b in the sera of NSCLC patients; (B) ROC curve of miR-19a/19b in stage I-III patients; (C) ROC curve of miR-19a/19b in stage IV patients. Abbreviations: NSCLC, non-small-cell lung cancer; ROC, receiver operating characteristic.

Nevertheless, miR-19a/19b can be used as a diagnostic marker for stage I-III NSCLC. If the test result is greater than 4.27, it is suggested to be stage I-III NSCLC. Test takers should perform further examinations to confirm or rule out such possibilities.

MiR-20a

The level of miR-20a in NSCLC patients was significantly downregulated in stage I, II, and III patients. In stage IV patients, it was markedly upregulated (Figure 5A). Similar to the previous method, the ROC curve of normal subjects and stage I-III patients and the ROC curve of normal subjects and stage IV patients could be plotted. Then, the interval of normal human ΔCt values could be determined.

The results showed that in the ROC curve of normal subjects and stage I-III patients, the AUC was 0.8975, and the best cut-off point was 3.425. The sensitivity and specificity of this value were 0.9020 and 0.7273, respectively (Figure 5B). In the ROC curve of normal subjects and stage IV patients, the AUC was 1.0000, and the best cut-off point was 0.01167. The sensitivity and specificity of this value were 1.0000 (Figure 5C).

Therefore, the ΔCt value interval of a normal person can be set to [0.01167, 3.425], and if the test result is less than 0.01167, it is suggested to be stage IV NSCLC; if the result is greater than 3.425, it is suggested to be stage I-III NSCLC.

MiR-92a-1

The expression level of miR-92a-1 in NSCLC patients showed no significant change in stage I. In stage II and III patients, it showed significant downregulation, and in stage IV patients, it showed marked upregulation (Figure 6A). The ROC curve of normal subjects and stage

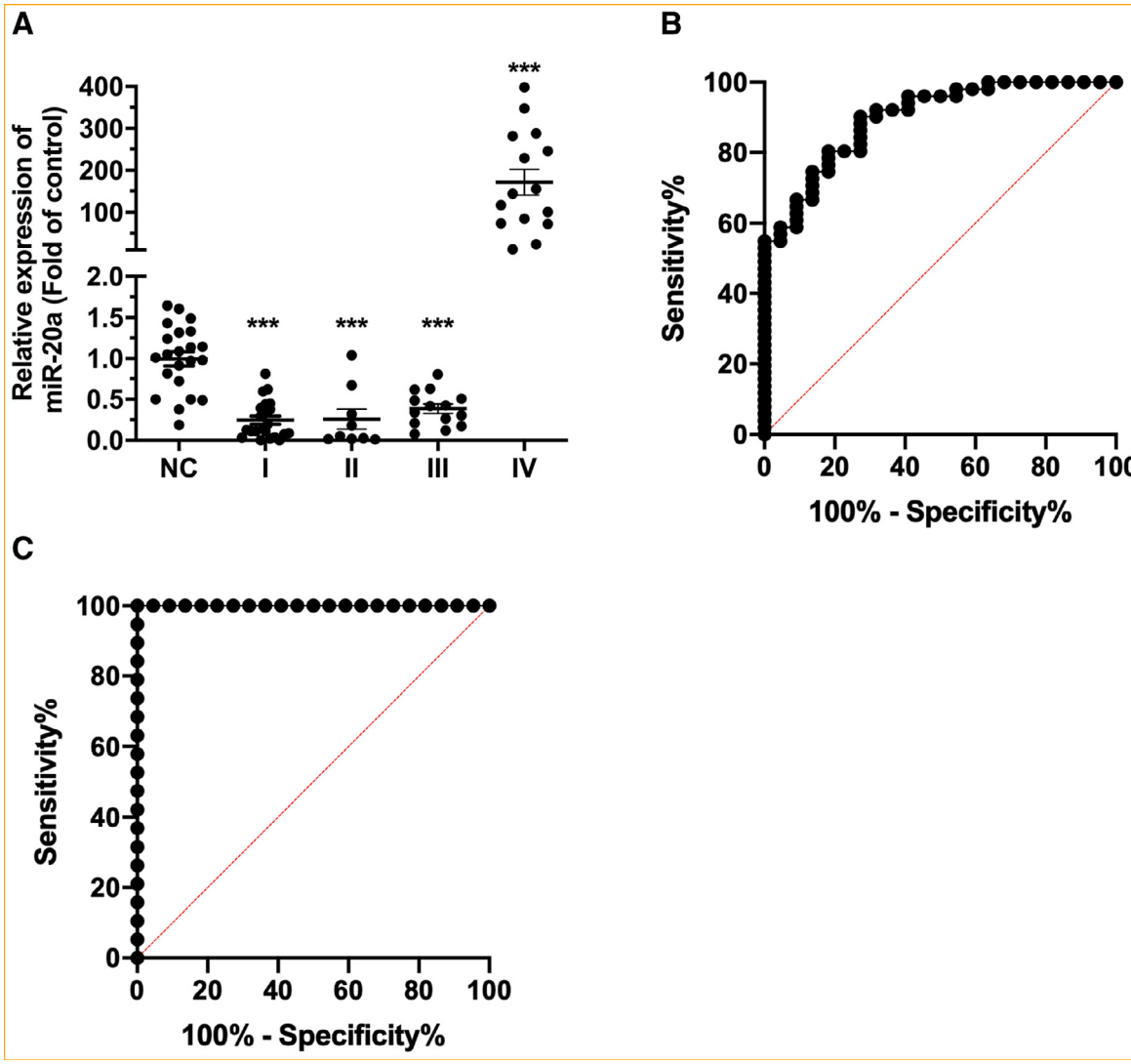

FIGURE 5. Expression level and ROC curve of miR-20a in the sera of NSCLC patients. (A) Expression level of miR-20a in the sera of NSCLC patients; (B) ROC curve of miR-20a in stage I-III patients; (C) ROC curve of miR-20a in stage IV patients. Abbreviations: NSCLC, non-small-cell lung cancer; ROC, receiver operating characteristic.

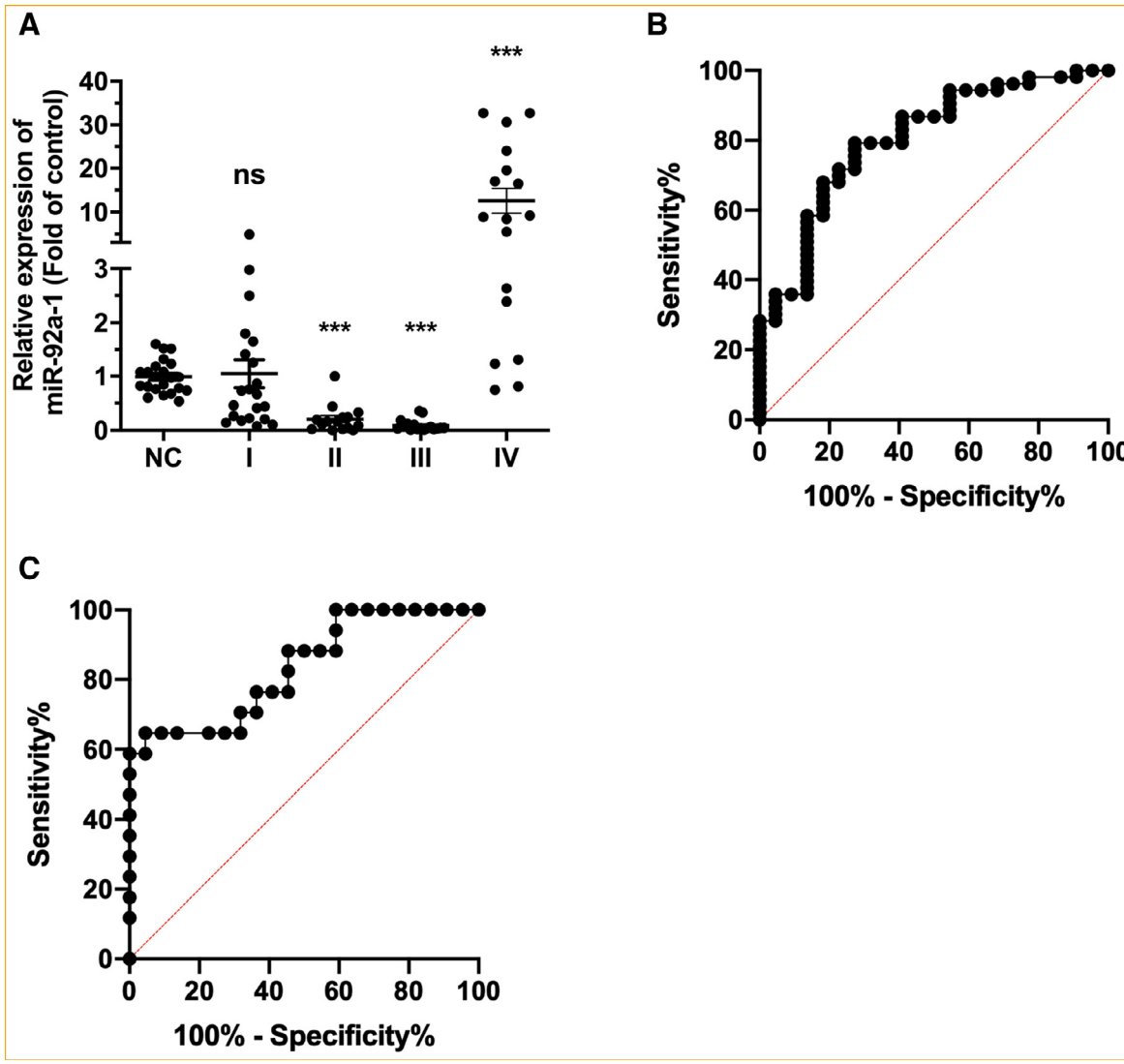

FIGURE 6. Expression level and ROC curve of miR-92a-1 in the sera of NSCLC patients. (A) Expression level of miR-92a-1 in the sera of NSCLC patients; (B) ROC curve of miR-92a-1 in stage I-III patients; (C) ROC curve of miR-92a-1 in stage IV patients. Abbreviations: NSCLC, non-small-cell lung cancer; ROC, receiver operating characteristic.

I-III patients and the ROC curve of normal subjects and stage IV patients could be plotted. Then, the interval of normal human ΔCt values could be determined.

The results showed that in the ROC curve of normal subjects and stage I-III patients, the AUC was 0.8097, and the best cut-off point was 6.852. The sensitivity and specificity of this value were 0.8302 and 0.5909, respectively (Figure 6B). In the ROC curve of normal subjects and stage IV patients, the AUC was 0.8342, and the best cut-off point was 5.342. The sensitivity and specificity of this value were 0.7647 and 0.6364, respectively (Figure 6C).

Therefore, the ΔCt value interval of a normal person can be set to [5.342, 6.852], and if the test result is less than 5.342, it is suggested to be stage IV NSCLC; if the result is greater than 6.852, it is suggested to be stage I-III NSCLC.

Sensitivity Statistics of Commonly Used Diagnostic Markers in NSCLC

The following diagnostic markers are used in the clinic: carbohydrate antigen 125 (Ca125), carcinoembryonic antigen (CEA), cytokeratin-19 fragment (CYFRA21-1), neuron-specific enolase (NSE), and squamous cell cancer antigen (SCCAG).[35]

This study collected data on these commonly used diagnostic markers from 74 patients with NSCLC (Table 2). The expression level of the miR-17-92 cluster in the sera of these patients was previously examined.

Table 3 was calculated from Table 2, and the overall diagnostic effects of the 6 miRNAs are shown in Table 4. It is apparent that both the sensitivity and specificity of the miRNAs were better than those of the current biomarkers used in the clinic.

TABLE 2. Sensitivity statistics of commonly used diagnostic markers in NSCLC.

	Stage I			Stage II		
	Positive	**Total**	**Sensitivity**	**Positive**	**Total**	**Sensitivity**
Ca125	11	28	0.3929	2	16	0.1250
CEA	1	28	0.0357	1	16	0.0625
CYFRA21-1	1	28	0.0357	2	16	0.1250
NSE	7	28	0.2500	3	16	0.1875
SCCAG	3	28	0.1071	2	16	0.1250
	Stage III			**Stage IV**		
	Positive	**Total**	**Sensitivity**	**Positive**	**Total**	**Sensitivity**
Ca125	6	14	0.4286	2	16	0.1250
CEA	4	14	0.2857	7	16	0.4375
CYFRA21-1	2	14	0.1429	2	16	0.1250
NSE	0	14	0.0000	1	16	0.0625
SCCAG	5	14	0.3571	3	16	0.1875

Abbreviations: Ca125, carbohydrate antigen 125; CEA, carcinoembryonic antigen; CYFRA21-1, cytokeratin-19 fragment; NSE, neuron-specific enolase; SCCAG, squamous cell cancer antigen.

TABLE 3. Sensitivity statistics of commonly used diagnostic markers in NSCLC (Stages I-III are combined).

	Stage I-III			Stage IV		
	Positive	**Total**	**Sensitivity**	**Positive**	**Total**	**Sensitivity**
Ca125	19	58	0.3276	2	16	0.1250
CEA	6	58	0.1035	7	16	0.4375
CYFRA21-1	5	58	0.0862	2	16	0.1250
NSE	10	58	0.1724	1	16	0.0625
SCCAG	10	58	0.1724	3	16	0.1875

Abbreviations: Ca125, carbohydrate antigen 125; CEA, carcinoembryonic antigen; CYFRA21-1, cytokeratin-19 fragment; NSE, neuron-specific enolase; SCCAG, squamous cell cancer antigen

TABLE 4. The overall diagnostic effects of the 6 miRNAs.

	Stage I-III			Stage IV			Interval of normal value (ΔCt)
	AUC	**Sensitivity**	**Specificity**	**AUC**	**Sensitivity**	**Specificity**	
miR-17	0.8097	0.8250	0.6818	1.000	1.000	1.000	[−0.1317, 3.085]
miR-18a	0.7388	0.8000	0.4737	0.9907	1.0000	0.8947	[2.620, 4.788]
miR-19a/19b	0.8451	0.7885	0.5556	0.5104	0.7500	0.4444	≧4.27
miR-20a	0.8975	0.9020	0.7273	1.0000	1.000	1.000	[0.01167, 3.425]
miR-92a-1	0.8097	0.8302	0.5909	0.8342	0.7647	0.6364	[5.342, 6.852]

A High Positive Correlation Between miR-17 and miR-20a

Based on the results above, we further analyzed whether there is a synchronization between miRNAs in the miR-17-92 cluster. The qRT-PCR data of patients in each stage were assessed, and the expression of miR-17 and miR-20a showed the same increasing and decreasing trends. Therefore, a correlation analysis between miR-17 and miR-20a was performed.

The correlation analysis showed that in patients with stage I and II disease, the Pearson correlation coefficient (r) was 0.9080 (Figure 7A). In patients with stage III and stage IV disease, this value was 0.9924 (Figure 7B). These results show that miR-17 is highly positively correlated with miR-20a expression. Therefore, it will be clinically more accurate to use miR-17 in combination with miR-20a for diagnosis.

MiR-17 and miR-20 as a 2-miRNA Panel for Stage I-III NSCLC Diagnosis

Since there is a high positive correlation between miR-17 and miR-20a, we then investigated whether these 2 miRNAs can be combined to improve the screening effect of stage I-III NSCLC. A prediction model was established by using binary logistic regression. This model combined miR-17 and miR-20a as a 2-miRNA panel, with the algorithm, ln (p/1-p) = −1.616 − 1.359 × miR-17 + 1.294 × miR-20a. According to the ROC curve plotted with this model, the

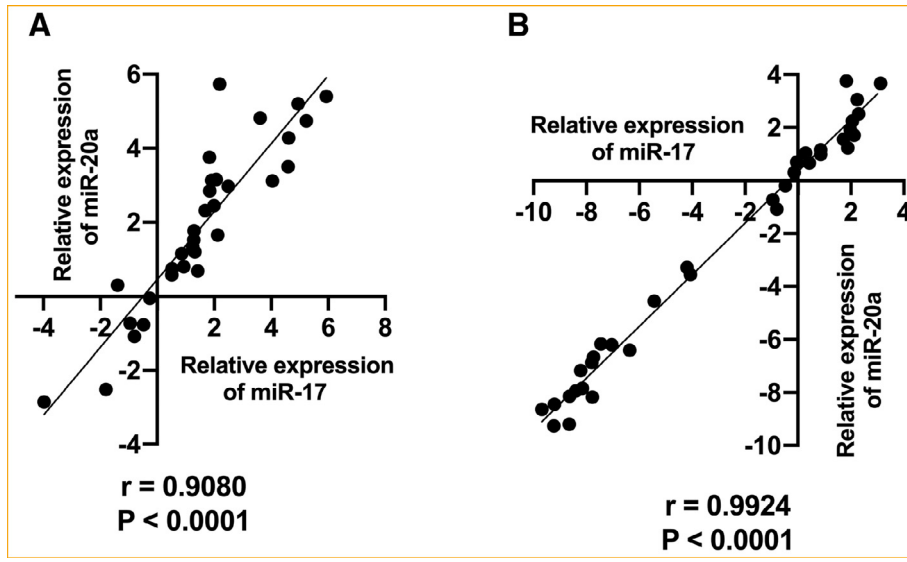

FIGURE 7. Positive correlation between miR-17 and miR-20a in the sera of patients with stage I/II and III/IV NSCLC. (A) Positive correlation between miR-17 and miR-20a in the sera of stage I/II NSCLC patients; (B) Positive correlation between miR-17 and miR-20a in the sera of stage III/IV NSCLC patients. Abbreviations: NSCLC, non-small-cell lung cancer; ROC, receiver operating characteristic.

AUC value reached 0.9479, which was higher than that of either of the 2 individual miRNAs (Figure 8). The best cut-off point was 0.6044. The sensitivity and specificity at this cut-off point were 0.9756 and 0.9090, respectively. These results indicated that this 2-miRNA panel is a stable marker for the diagnosis of NSCLC patients.

The MiR-17-92 Cluster has High Expression Levels in NSCLC Cell Lines

For further research, qRT-PCR was utilized to detect the expression level of the miRNAs in normal cell lines and NSCLC cell lines.[25]

In this study, human bronchial epithelial cells (BEAS-2B) were used as a control. The NSCLC cell lines used in this study were A549, H1299, HCC827, PC-9 and 95-D. The results indicated that the miRNAs of the miR-17-92 gene cluster in the NSCLC cell lines showed significantly higher expression compared to that in BEAS-2B (Figure 9).

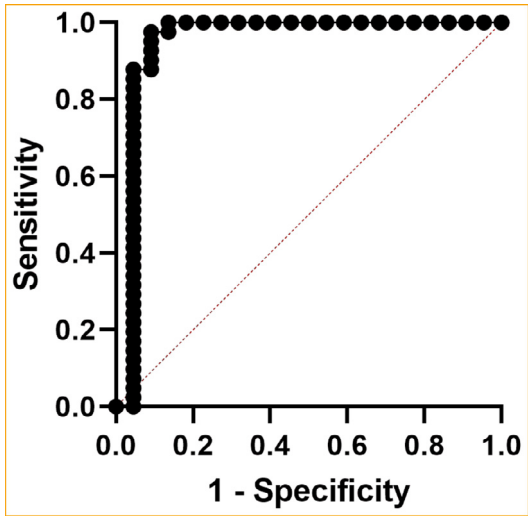

FIGURE 8. ROC Curve of the 2-miRNA panel in stage I-III patients. Abbreviation: ROC, receiver operating characteristic.

DISCUSSION

As mentioned in the introduction, NSCLC, the dominant type of lung cancer, seriously threatens human health.[33] The 5-year survival rate of early-stage NSCLC is more than 90%, while this value is only 15% in late-stage NSCLC.[36] Nevertheless, the detection rate of early-stage NSCLC is low, partly because early-stage NSCLC has almost no or slight symptoms. Patients tend to ignore these symptoms and thus miss the best opportunity to receive treatment.

Another reason is the lack of means to conduct an early diagnosis of lung cancer. Low-dose spiral computed tomography has been reported to effectively screen early-stage NSCLC.[37] However, this method has disadvantages, such as potentially harmful radiation and high costs.[38] Therefore, a relatively low cost and harmless method should be discovered to provide screening for early-stage NSCLC in a wide range of populations.

Circulating miRNAs in serum may be a promising marker for early diagnostics in NSCLC. It has several advantages. First, serum can be obtained in an easier way. Second, its costs are more affordable. Last, circulating miRNAs show characteristics such as tissue specificity, high conservation and changes with time.

Various studies have revealed that some circulating miRNAs have the potential to be used as diagnostic markers. Huang et al suggested that 6 serum-based miRNAs have the potential to be diagnostic markers for gastric cancer.[39] Wang et al found that 5 miRNAs, including

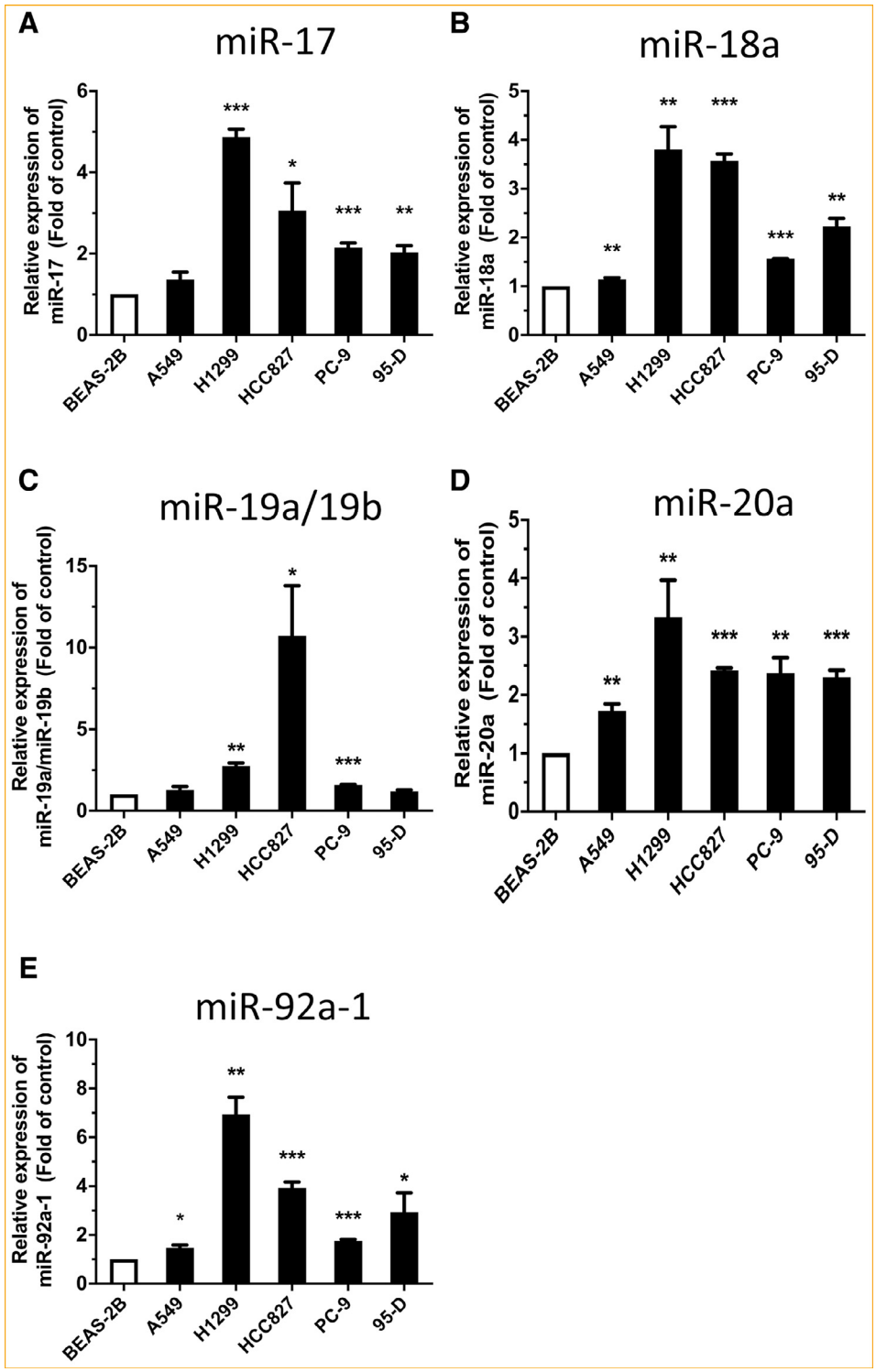

FIGURE 9. Expression of the miR-17-92 gene cluster in NSCLC cell lines. (A-E) Expression levels of miR-17 (A), miR-18a (B), miR-19a/19b (C), miR-20a (D) and miR-92a-1 (E) in NSCLC cell lines. Abbreviations: NSCLC, non-small-cell lung cancer.

miR-205a-5p, miR-145-5p, miR-10a-5p, miR-346 and miR-328-3p, were more highly expressed in ovarian cancer and thus can be used as diagnostic markers.[40] Yang et al reported that a 4-miRNA panel is effective in diagnosing NSCLC.[18] These studies all confirmed that circulating miRNAs could be diagnostic markers.

However, miRNAs in serum have to be processed via multiple procedures to perform a qRT-PCR test, which

will take a relatively long time if conducted manually. This problem also exists in the diagnosis of people who are suspected to have COVID-19, a disease caused by the novel coronavirus SARS-CoV-2, in China. Since qRT-PCR is the only way to make a definite diagnosis, a large number of people are waiting to be tested. However, the testing itself takes time, and patients' symptoms sometimes worsen in the waiting period, resulting in the death of some patients. Under such circumstances, some hospitals have introduced an automatic nucleic acid purification and fluorescent PCR analysis system, which was developed by Xiamen Amplly Bioengineering Co., Ltd. With proper kits, this machine can execute the procedure from sample preparation to genetic testing automatically, which improves the testing efficiency greatly and reduces human errors.

When labs are equipped with more similar instruments, qRT-PCR tests can become routine tests like complete blood counts. In addition, with the large-scale application of this method, the unit price of a single test can be affordable.

For the 6 individual miRNAs in the miR-17-92 gene cluster, the effects as diagnostic markers for NSCLC are ranked in the following order: miR-20a, miR-17, miR-18a, miR-92a-1 and miR-19a/19b. In addition, miR-17 and miR-20a had relatively higher concentrations in serum, and the number of cycles in qRT-PCR was less than those of the other miRNAs. Therefore, as a diagnostic marker, it can be more accurately quantified and reduce experimental errors. Moreover, based on the high positive correlation between miR-17 and miR-20a expression, these 2 miRNAs can be used together as a panel to improve the accuracy of the diagnostic process.

Past studies have revealed that the regulatory mechanism of the miR-17-92 gene cluster in cancers is complicated, sometimes even contradictory. For example, Zhu et al confirmed that miR-17 is overexpressed in pancreatic cancer,[41] while Lin et al asserted that it is downregulated in NSCLC.[42] In our study, we confirmed that even in the same type of cancer, the expression levels can also be distinct in tumor progression. The data obtained indicated a trend that the expression level of this gene cluster first decreased in stage I-III. The lowest expression level appeared in stage II (miR-17, miR-18a, miR-19a/19b, and miR-20a) and stage III (miR-92a-1). Then, in stage IV, the expression levels of all 6 miRNAs rose to varying degrees. Among them, miR-17 and miR-20a increased sharply. We speculate that in stage I-III, the expression of the 6 miRNAs is inhibited to different degrees. In stage IV, such inhibitions are relieved. The unusually high expression of this gene cluster in stage IV may also indicate that this gene cluster is associated with tumor metastasis, since stage IV patients often have distant metastasis. However, this hypothesis requires further research.

Other studies related to diagnostic markers usually set one cut-off point for each miRNA, while our study set the interval of normal humans, which had 2 cut-off points. This is because we discovered that the miR-17-92 gene cluster was often downregulated in stage I-III NSCLC and markedly upregulated in stage IV NSCLC. The expression pattern of this gene cluster enabled us to distinguish patients from different stages of NSCLC, which was a unique superiority compared to other miRNAs.

Studies concerning diagnostic markers usually include 2 phases, the training phase and validation phase. Because of the lack of serum samples, the validation phase has yet to be carried out. More serum samples need to be collected and further investigated.

CONCLUSIONS

MiR-17 and miR-20a in the miR-17-92 cluster may be promising markers for screening NSCLC. Moreover, the combination of these 2 miRNAs has a better effect than using them individually. Further studies with more clinical samples and more sensitive methods are needed to expand the quantity of samples to further confirm these results. Afterward, the results will be able to be used as diagnostic markers in the future.

AUTHOR CONTRIBUTIONS

Z.M. proposed the concept; Q.S. and J.Z. collected patient sera and determined their pathological characteristics; C.Y. and X.J. developed the methodology, conducted experiments, and collected and analyzed data; C. Y. wrote the manuscript; Z.M. administered the whole project and revised the manuscript.

ACKNOWLEDGMENTS

The authors would give great thanks to Dr. Yanli Li and Yang Shao for their constructive discussions and Nanxiang Mao for his assistance in the experiments.

SUPPLEMENTARY MATERIALS

Supplementary material associated with this article can be found, in the online version, at https://doi.org/10.1016/j.amjms.2020.05.004.

REFERENCES

1. **Siegel RL, Miller KD, Jemal A.** Cancer statistics, 2019. *CA Cancer J Clin*. 2019;69:7–34.
2. **Wood SL, Pernemalm M, Crosbie PA, et al.** Molecular histology of lung cancer: from targets to treatments. *Cancer Treat Rev*. 2015;41:361–375.
3. **Bray F, Ferlay J, Soerjomataram I, et al.** Global cancer statistics 2018: GLOBOCAN estimates of incidence and mortality worldwide for 36 cancers in 185 countries. *CA Cancer J Clin*. 2018;68:394–424.
4. **Wood DE, Kazerooni EA, Baum SL, et al.** Lung cancer screening, version 3.2018, NCCN clinical practice guidelines in oncology. *J Natl Compreh Cancer Netw*. 2018;16:412–441.
5. **Bartel DP.** MicroRNAs: genomics, biogenesis, mechanism, and function. *Cell*. 2004;116:281–297.

6. **Jung A, Kirchner T.** Liquid biopsy in tumor genetic diagnosis. *Deutsches Arzteblatt International*. 2018;115:169–174.
7. **Fang LL, Wang XH, Sun BF, et al.** Expression, regulation and mechanism of action of the miR-17-92 cluster in tumor cells. *Int J Mol Med*. 2017;40:1624–1630.
8. **Jun L, Gad G, Miska EA, et al.** MicroRNA expression profiles classify human cancers. *Nature*. 2005;435:834–838.
9. **Shuibin L, Gregory RI.** MicroRNA biogenesis pathways in cancer. *Nat Rev Cancer*. 2015;15:321–333.
10. **Lu S, Hui K, Hou Y, et al.** Two plasma MicroRNA panels for diagnosis and subtype discrimination of lung cancer. *Lung Cancer*. 2018;123: 44–51.
11. **Mitchell PS, Parkin RK, Kroh EM, et al.** Circulating microRNAs as stable blood-based markers for cancer detection. *Proc Natl Acad Sci U S A*. 2008;105:10513–10518.
12. **Manel E.** Non-coding RNAs in human disease. *Nat Rev Genet*. 2011;12:861–874.
13. **Li H, Wu Q, Li T, et al.** The miR-17-92 cluster as a potential biomarker for the early diagnosis of gastric cancer: evidence and literature review. *Oncotarget*. 2017;8:45060–45071.
14. **Foshay KM, Gallicano GI.** miR-17 family miRNAs are expressed during early mammalian development and regulate stem cell differentiation. *Dev Biol*. 2009;326:431–443.
15. **Zhang X, Li Y, Qi P, et al.** Biology of MiR-17-92 cluster and its progress in lung cancer. *Int J Med Sci*. 2018;15:1443–1448.
16. **Mendell JT.** miRiad roles for the miR-17-92 cluster in development and disease. *Cell*. 2008;133:217–222.
17. **Hayashita Y, Osada H, Tatematsu Y, et al.** A polycistronic microRNA cluster, miR-17-92, is overexpressed in human lung cancers and enhances cell proliferation. *Cancer Res*. 2005;65:9628–9632.
18. **Yang X, Zhang Q, Zhang M, et al.** Serum microRNA signature is capable of early diagnosis for non-small cell lung cancer. *Int J Biol Sci*. 2019;15:1712–1722.
19. **Ventura A, Young AG, Winslow MM, et al.** Targeted deletion reveals essential and overlapping functions of the miR-17 through 92 family of miRNA clusters. *Cell*. 2008;132:875–886.
20. **Zhang Y, Zhang Y, Yin Y, et al.** Detection of circulating exosomal miR-17-5p serves as a novel non-invasive diagnostic marker for non-small cell lung cancer patients. *Pathol-Res Pract*. 2019;215:152466.
21. **Liu F, Cheng L, Xu J, et al.** miR-17-92 functions as an oncogene and modulates NF-kappaB signaling by targeting TRAF3 in MGC-803 human gastric cancer cells. *Int J Oncol*. 2018;53:2241–2257.
22. **Jia Q, Sun H, Xiao F, et al.** miR-17-92 promotes leukemogenesis in chronic myeloid leukemia via targeting A20 and activation of NF-kappaB signaling. *Biochem Biophys Res Commun*. 2017;487:868–874.
23. **Zhou P, Ma L, Zhou J, et al.** miR-17-92 plays an oncogenic role and conveys chemo-resistance to cisplatin in human prostate cancer cells. *Int J Oncol*. 2016;48:1737–1748.
24. **Liang C, Zhang X, Wang HM, et al.** MicroRNA-18a-5p functions as an oncogene by directly targeting IRF2 in lung cancer. *Cell Death Dis*. 2017;8: e2764.
25. **Leidinger P, Brefort T, Backes C, et al.** High-throughput qRT-PCR validation of blood microRNAs in non-small cell lung cancer. *Oncotarget*. 2016;7:4611–4623.
26. **Bianchi F, Nicassio F, Marzi M, et al.** A serum circulating miRNA diagnostic test to identify asymptomatic high−risk individuals with early stage lung cancer. *Embo Mol Med*. 2011;3:495–503.
27. **Wang L, Wang D, Zheng G, et al.** Clinical evaluation and therapeutic monitoring value of serum tumor markers in lung cancer. *Int J Biol Markers*. 2016;31:e80–e87.
28. **Jensen SG.** Evaluation of two commercial global miRNA expression profiling platforms for detection of less abundant miRNAs Bmc. *Genomics*. 2011;12:435.
29. **Zhibin H, Xi C, Yang Z, et al.** Serum microRNA signatures identified in a genome-wide serum microRNA expression profiling predict survival of non-small-cell lung cancer. *J Clin Oncol*. 2016;28:1721–1726.
30. **Mestdagh P, Vlierberghe PV, An DW, et al.** A novel and universal method for microRNA RT-qPCR data normalization. *Genome Biol*. 2009;10:R64.
31. **Zhou X, Zhu W, Li H, et al.** Diagnostic value of a plasma microRNA signature in gastric cancer: a microRNA expression analysis. *Sci Rep*. 2015;5:11251.
32. **Livak KJ, Schmittgen TD.** Analysis of relative gene expression data using real-time quantitative PCR and the $2^{-\Delta\Delta C T}$ method. *Methods*. 2001;25:402–408.
33. **Sourvinou IS, Markou A, Lianidou ES.** Quantification of circulating miRNAs in plasma : effect of preanalytical and analytical parameters on their isolation and stability. *J Mol Diagn*. 2013;15:827–834.
34. **Matin F, Jeet V, Moya L, et al.** A plasma biomarker panel of four MicroRNAs for the diagnosis of prostate. *Cancer Sci Rep*. 2018;8:6653.
35. **Chen Z-q, Huang L-s, Zhu B.** Assessment of seven clinical tumor markers in diagnosis of non-small-cell lung. *Cancer Dis Markers*. 2018;2018:9845123.
36. **Detterbeck FC.** The eighth edition TNM stage classification for lung cancer: what does it mean on main street? *J Thorac Cardiovasc Surg*. 2018;2018:9845123.
37. **Koning HJ, De RM, Plevritis SK, et al.** Benefits and harms of computed tomography lung cancer screening strategies: a comparative modeling study for the U.S. Preventive Services Task Force. *Ann Intern Med*. 2014;160:311–320.
38. **Chu GCW, Lazare K, Sullivan F.** Serum and blood based biomarkers for lung cancer screening: a systematic review. *BMC Cancer*. 2018;18:181.
39. **Huang Z, Zhu D, Wu L, et al.** Six serum-based miRNAs as potential diagnostic biomarkers for gastric cancer. *Cancer Epidemiol Biomarkers Prev*. 2017;26:188–196.
40. **Wang W, Yin Y, Shan X, et al.** The value of plasma-based MicroRNAs as diagnostic biomarkers for ovarian cancer. *Am J Med Sci*. 2019;358:256–267.
41. **Zhu Y, Gu J, Li Y, et al.** MiR-17-5p enhances pancreatic cancer proliferation by altering cell cycle profiles via disruption of RBL2/E2F4-repressing complexes. *Cancer Lett*. 2018;412:59–68.
42. **Lin S, Sun JG, Wu JB, et al.** Aberrant microRNAs expression in CD133 (+)/CD326(+) human lung adenocarcinoma initiating cells from A549. *Mol Cells*. 2012;33:277–283.

Submitted September 24, 2019; accepted May 2, 2020.

Conflict of interest: All authors declare no conflicts of interest.

Source of funding: This work was supported by the Nurture Projects for Basic Research of Shanghai Chest Hospital (2018YNJCM06) and State Key Laboratory of Cell Biology, Institute of Biochemistry and Cell Biology, Chinese Academy of Sciences.

Correspondence: Zhongliang Ma, PhD, Lab for Noncoding RNA & Cancer, School of Life Sciences, 99 Shangda Road, Shanghai University, Shanghai, China, 200444. (E-mail: zlma@shu.edu.cn).

Correspondence: Qiangling Sun, PhD, Department of Thoracic Surgery, Thoracic Cancer Institute, Shanghai Chest Hospital Affiliated to Shanghai Jiao Tong University, 241 West Huaihai Road, Shanghai, China, 200030. (E-mail: shqling@163.com).